Title

Water-soluble drug partitioning and adsorption in HEMA/MAA hydrogels

Journal

Biomaterials, 35(2)

ISSN

0267-6605

Authors

Dursch, Thomas J

Taylor, Nicole O

Liu, David E

et al.

Publication Date

2014

DOI

10.1016/j.biomaterials.2013.09.109

Peer reviewed

Biomaterials 35 (2014) 620–629

Contents lists available at ScienceDirect

Biomaterials

journal homepage: www.elsevier.com/locate/biomaterials

Water-soluble drug partitioning and adsorption in HEMA/MAA hydrogels

Thomas J. Dursch [a], Nicole O. Taylor [a], David E. Liu [a], Rong Y. Wu [a], John M. Prausnitz [a], Clayton J. Radke [a,b,*]

[a] Chemical and Biomolecular Engineering Department, University of California, Berkeley, CA 94720, United States
[b] Vision Science, School of Optometry, University of California, Berkeley, CA 94720, United States

ARTICLE INFO

Article history:
Received 21 August 2013
Accepted 26 September 2013
Available online 20 October 2013

Keywords:
Drug
Partition coefficient
Hydrogel
HEMA/MAA
Fluorescence confocal microscopy
Back extraction

ABSTRACT

Two-photon confocal microscopy and back extraction with UV/Vis-absorption spectrophotometry quantify equilibrium partition coefficients, k, for six prototypical drugs in five soft-contact-lens-material hydrogels over a range of water contents from 40 to 92%. Partition coefficients were obtained for acetazolamide, caffeine, hydrocortisone, Oregon Green 488, sodium fluorescein, and theophylline in 2-hydroxyethyl methacrylate/methacrylic acid (HEMA/MAA, $pK_a \approx 5.2$) copolymer hydrogels as functions of composition, aqueous pH (2 and 7.4), and salinity. At pH 2, the hydrogels are nonionic, whereas at pH 7.4, hydrogels are anionic due to MAA ionization. Solute adsorption on and nonspecific electrostatic interaction with the polymer matrix are pronounced. To express deviation from ideal partitioning, we define an enhancement or exclusion factor, $E \equiv k/\phi_1$, where ϕ_1 is hydrogel water volume fraction. All solutes exhibit $E > 1$ in 100 wt % HEMA hydrogels owing to strong specific adsorption to HEMA strands. For all solutes, E significantly decreases upon incorporation of anionic MAA into the hydrogel due to lack of adsorption onto charged MAA moieties. For dianionic sodium fluorescein and Oregon Green 488, and partially ionized monoanionic acetazolamide at pH 7.4, however, the decrease in E is more severe than that for similar-sized nonionic solutes. Conversely, at pH 2, E generally increases with addition of the nonionic MAA copolymer due to strong preferential adsorption to the uncharged carboxylic-acid group of MAA. For all cases, we quantitatively predict enhancement factors for the six drugs using only independently obtained parameters. In dilute solution for solute i, E_i is conveniently expressed as a product of individual enhancement factors for size exclusion (E_i^{ex}), electrostatic interaction (E_i^{el}), and specific adsorption (E_i^{ad}) : $E_i \equiv E_i^{ex}\, E_i^{el}\, E_i^{ad}$. To obtain the individual enhancement factors, we employ an extended Ogston mesh-size distribution for E_i^{ex}; Donnan equilibrium for E_i^{el}; and Henry's law characterizing specific adsorption to the polymer chains for E_i^{ad}. Predicted enhancement factors are in excellent agreement with experiment.

1. Introduction

Hydrogels are cross-linked polymeric networks that readily imbibe water and swell without dissolving [1–7]. Because of their soft consistency, high water content, and biocompatibility, hydrogels are used in numerous biomedical and pharmaceutical applications, including: drug delivery [8,9], bioseparations [10,11], and soft-contact lenses [12–14]. The effectiveness of these applications is dictated, in large part, by the solubilities of aqueous solutes in hydrogels. Accordingly, a key hydrogel characteristic is the equilibrium partition coefficient, k_i, of a dilute solute i Refs. [1,12,15] defined by

$$k_i \equiv C_i^{gel}/C_i^{bulk} \tag{1}$$

where C_i^{gel} is the concentration of solute in the hydrogel per unit volume of swollen hydrogel and C_i^{bulk} is the corresponding solute concentration in the external aqueous solution equilibrated with the hydrogel. Eq. (1) strictly applies for reversible equilibrium solute partitioning. Further, the partition coefficient is independent of bulk aqueous solute concentration only in dilute solution where solute molecules do not interact with each other [1,2].

For point solutes that do not interact with the polymer network, k_i equals the hydrogel water volume fraction, ϕ_1. It is, therefore, useful to define an enhancement (or exclusion) factor E_i by Ref. [1]

* Corresponding author. Chemical and Biomolecular Engineering Department, University of California, 101E Gilman, Berkeley, CA 94720-1462, United States. Tel.: +1 510 642 5204; fax: +1 510 642 4778.
E-mail address: radke@berkeley.edu (C.J. Radke).

0142-9612/$ – see front matter © 2013 Elsevier Ltd. All rights reserved.
http://dx.doi.org/10.1016/j.biomaterials.2013.09.109

$$E_i \equiv k_i/\phi_1. \quad (2)$$

For solutes that are partially rejected from the hydrogel, $E_i < 1$, whereas $E_i > 1$ occurs only for favorable solute interaction with the internal polymer network (e.g., through specific adsorption or ion binding). $E_i = 1$ corresponds either to ideal partitioning or to apparent ideal partitioning arising from compensation between exclusion and enhancement. $E_i = 0$ indicates a solute too large to penetrate the water-filled pockets of the hydrogel network.

When the aqueous solution is dilute, it is reasonable to assume additivity of the separate free energies arising from different molecular contributions. Appendix A demonstrates that the resulting enhancement factor for solute i is the product of individual enhancement factors

$$E_i \equiv E_i^{ex}\, E_i^{el}\, E_i^{ad} \quad (3)$$

where E_i^{ex} designates hard-sphere size exclusion, E_i^{el} denotes nonspecific electrostatic interaction, and E_i^{ad} indicates specific solute adsorption on polymer strands. Thus, whether E_i is greater or less than unity depends on combinations of the various solute/hydrogel enhancement factors. $E_i < 1$ reflects partial rejection due to size exclusion ($E_i^{ex} < 1$) and/or repulsive electrostatic interaction ($E_i^{el} < 1$). For nonionic ($E_i^{el} = 1$) or counterion ($E_i^{el} > 1$) solutes, $E_i < 1$ arises solely due to size exclusion. Because large solutes access only a fraction of the water-filled space, E_i approaches zero as solute size increases [1]. If solutes complex specifically with the polymer chains ($E_i^{ad} > 1$), $E_i < 1$ results from competition between severe size exclusion and favorable adsorption. For non-adsorbing solutes, however, $E_i^{ad} = 1$. Coion solutes ($E_i^{el} < 1$), exhibit $E_i < 1$ because of both size exclusion and electrostatic repulsion. In this case, as solute charge or hydrogel charge density increases, electrostatic repulsion increases ($E_i^{el} << 1$), and E_i tends towards zero.

For counterion solutes, $E_i > 1$ diagnoses favorable electrostatic interaction and possibly specific adsorption offsetting partial rejection from size exclusion. Similarly, for nonionic and coion solutes, $E_i > 1$ arises only when adsorption overcomes size exclusion and/or electrostatic repulsion. When solutes are large (relative to the average mesh size) or for strong electrostatic repulsion, $E_i > 1$ results only from strong complexation with polymer strands. Solutes may adsorb reversibly ($E_i^{ad} > 1$) or irreversibly ($E_i^{ad} >> 1$) on the interior hydrogel network, and in some cases, also adsorb to the hydrogel exterior surface [13]. Because of the wide variety of applications and because observed enhancement factors vary widely [1,5,7,12–31], significant effort has been expended toward obtaining solute equilibrium partition coefficients, often by back extraction [12,15,16,24,27] using UV/Vis-absorption spectrophotometry [18,22,24,25].

Published work falls primarily into three classes: (1) $E_i < 1$ solely due to size exclusion [1,5,7,12,13,20,21,23,28–30]; (2) $E_i < 1$ resulting from size exclusion and Donnan electrostatic repulsion [12,17–19]; and (3) $E_i > 1$ where solutes interact specifically with the polymer chains [2,13–18,22,24–27]. The first class consists of small nonionic solutes, such as small sugars and non-adsorbing drugs, and larger nonionic solutes, including polymers and proteins. Solutes in the second class are typically coions, both small (e.g., salts and fluorescent dyes) and large (e.g., proteins and polymeric surfactants). The third class includes counterion solutes (e.g., polymeric surfactants and proteins) and specifically adsorbing nonionic solutes, such as drugs and polymers. Most systems studied [1,2,5,7,12–18,20–30] fall into the first or third class. For systems where prediction of k_i is attempted, however, nearly all fall into the first class (i.e., $E_i < 1$) [1,5,7,17,19–21,23]. $E_i > 1$ is often exhibited by polymers, polymeric surfactants, and proteins in soft-contact-lens materials [1,2,13,16–20] and by ionic/nonionic drugs and vitamins in drug-delivery hydrogels [14,15,21–30]. Quantifying the effects of specific adsorption and nonspecific electrostatic interaction on equilibrium solute partitioning is critical for data interpretation.

This work reports experimental and theoretically predicted solute enhancement factors in hydrogels where specific adsorption is pronounced. Attention is given to hydrogels representative of soft-contact-lens materials that have relatively high polymer content and are sometimes partially ionic [1,2,12–14]. The hydrogels studied are copolymers of 2-hydroxyethyl methacrylate (HEMA) and anionic (for pH > 5.2) methacrylic acid (MAA) over a large range of water content. We employ two-photon laser-scanning confocal microscopy and back extraction with UV/Vis spectrophotometry. Partition coefficients are obtained for small ionic and nonionic water-soluble drugs as functions of pH, hydrogel composition, and aqueous salinity. Solute sizes are determined from independent measurement of bulk aqueous diffusion coefficients in a restricted diffusion cell and Stokes–Einstein theory. Enhancement factors are predicted for six solutes (acetazolamide, caffeine, hydrocortisone, Oregon Green 488, sodium fluorescein, and theophylline) in five different water-content hydrogels accounting for hard-sphere size exclusion, Donnan electrostatic repulsion, and specific adsorption. Predictions are based on independently measured parameters, and not on correlation of the experimental partition coefficients.

2. Materials and methods

2.1. Chemicals

Sigma Aldrich (St. Louis, MO) provided all monomers and chemicals used in hydrogel synthesis: 2-hydroxyethyl methacrylate (97%, HEMA, Cat. No. 128635-500G), methacrylic acid (99%, MAA, Cat. No. 155721-500G), ethylene glycol dimethacrylate (98%, EGDMA, Cat. No. 335681-100 ML), 4,4′-azobis (4-cyanovaleric acid) (98+ %, 11590-100G), and Sigmacote (SL2-100 ML), the latter used to hydrophobize glass-mold surfaces prior to polymerization. Following free-radical polymerization, hydrogels were swollen or deswollen in pH 7.4 or 2, respectively. To prepare a pH = 7.4 phosphate buffer saline solution (PBS: 0.15 M NaCl, 0.017 M $Na_2HPO_4 \cdot 7H_2O$, and 0.003 M $NaH_2PO_4 \cdot H_2O$), sodium phosphate dibasic heptahydrate ($Na_2HPO_4 \cdot 7H_2O$, 99+ %, SX0715-1), sodium phosphate monobasic monohydrate ($NaH_2PO_4 \cdot H_2O$, 98%, SX0710-1), and sodium chloride (NaCl, 99.8+ %, SX0425-1), purchased from EMD Chemicals Inc. (Darmstadt, Germany), were dissolved in distilled/deionized (DI) water. To prepare a pH = 2 hydrochloric acid solution (HCl: 0.15 M NaCl and 0.02 M HCl), hydrochloric acid (HCl, 0.1 N, Cat. No. 38280-1EA), purchased from Sigma Aldrich, and NaCl were mixed with DI water.

Solutes purchased from Sigma Aldrich include: theophylline (99+ %, Cat. No. T1633-50G), caffeine (99+ %, Cat. No. C0750-5G), acetazolamide (99+ %, Cat. No. A6011-10G), hydrocortisone (98+ %, Cat. No. H4001-5G), and fluorescein sodium salt (99+ %, Cat. No. F-6377-100G). 2′7′-Difluorofluorescein (Oregon Green 488, 97%, Cat. No. D-6145-10MG) was purchased from Life Technologies (Grand Island, NY, USA). Aqueous theophylline, caffeine, and hydrocortisone are nonionic over the studied pH range. At pH 7.4, sodium fluorescein and Oregon Green 488 are dianionic [31], and acetazolamide is monoanionic and partially ionized [32]. At pH 2, all solutes are neutral. All chemicals were used without further purification. Partitioning and diffusion experiments were performed at ambient temperature.

2.2. Hydrogel synthesis

Following Kotsmar et al. [1], HEMA/MAA hydrogels were synthesized by simultaneous copolymerization and cross-linking of monomers in aqueous solution with EGDMA as the cross-linking agent [1,2,25]. Solutions consisted of varying HEMA:MAA ratio (100:0, 99:1, 90:10, 70:30, and 0:100), 0.25 wt % EGDMA, 0.5 wt % 4,4′-azobis(4-cyanovaleric acid), and 30 wt % DI water. Hydrogels are referred to by their corresponding wt % MAA, where wt % MAA and wt % HEMA sum to 100. All percentages are of total monomer. The reaction mixture was magnetically stirred until complete dissolution of the thermoinitiator. Nitrogen gas was bubbled through the reaction mixture for 15 min to remove dissolved oxygen, resulting in less than 1% change in HEMA:MAA composition. The bubbled reaction mixture was injected between two upright glass plates previously hydrophobized with Sigmacote and separated by a 100 or 250-μm spacer. Free-radical thermally initiated polymerization took place in an oven whose temperature was raised from 60 to 90 °C over a 60-min period and then maintained at 90 °C for 60 min. When cooled, hydrogels were boiled in DI water for 45 min to remove unreacted monomer.

Table 1
Hydrogel water volume fractions with varying HEMA:MAA weight ratios.

Hydrogel composition (HEMA:MAA)	ϕ_1 (in PBS)	ϕ_1 (in HCl)
100:0	0.43 ± 0.02	0.40 ± 0.01
99:1	0.54 ± 0.02	0.39 ± 0.01
90:10	0.77 ± 0.04	0.29 ± 0.01
70:30	0.83 ± 0.02	0.31 ± 0.02
0:100	0.92 ± 0.01	0.71 ± 0.07

2.3. Equilibrium water content

Hydrogel equilibrium water content, or water volume fraction, ϕ_1, was determined gravimetrically following Guan et al. [12]. 9-mm-diameter discs were bored into synthesized hydrogel slabs and placed into either PBS buffer or HCl solutions. Solutions were changed daily for a minimum of 3 d to ensure equilibration with the surrounding solution. To determine water content, equilibrated hydrogels were removed from solution, lightly blotted with Fisherbrand® weighing paper (Fisher Scientific, Pittsburgh, PA), and weighed (m_{wet}). Hydrogels were then placed in an oven at 70 °C overnight and ambient-temperature dry-hydrogel mass (m_{dry}) was used to calculate water content by

$$\phi_1 = \frac{\rho_{wet}}{\rho_1}\left[\frac{m_{wet} - m_{dry}}{m_{wet}}\right], \quad (4)$$

where ρ is mass density and subscripts 1, wet, and dry denote water, swollen hydrogel, and dry hydrogel, respectively. Since $\rho_1 \approx \rho_{wet}$ (to within 5%), ϕ_1 in Eq. (4) is approximately weight fraction. Table 1 reports measured ϕ_1 for the HEMA/MAA hydrogels equilibrated in either PBS (pH 7.4) or HCl (pH 2), where hydrogel composition varied from 0 to 100 wt % MAA. Each water-content measurement was repeated at least three times. At pH 7.4 (PBS), hydration of charged carboxylic groups swells the MAA-containing hydrogels from 55 to 90% water, for gels containing 1 and 100 wt % MAA, respectively. At pH 2 (HCl), addition of MAA initially (1–50 wt %) results in hydrogel deswelling likely due to interstrand hydrogen bonding between uncharged MAA and HEMA monomers [33]. Further addition of MAA (beyond 50 wt %), however, significantly increases hydrogel water content, because hydration of hydrophilic uncharged MAA moieties overcomes interchain hydrogen bonding.

2.4. Solute loading

Swollen hydrogels were soaked for a minimum of 2 d in 50 and 20-mL solute solutions (i.e., volume ratio of solution to hydrogel was 250) at pH 7.4 and 2, respectively. Initial loading concentrations for sodium fluorescein and Oregon Green 488 were 1×10^{-5} M and 1×10^{-7} M in PBS and HCl solutions, respectively. Initial loading concentrations for theophylline and caffeine, acetazolamide, and hydrocortisone were 6×10^{-3} M, 2×10^{-3} M, and 2×10^{-4} M, respectively, in both PBS and HCl. In this concentration range, ϕ_1 was unaffected by solute loading. To confirm that the hydrogels were fully loaded, solute uptake time was varied from 2 to 7 d, resulting in less than 4% change in solute partition coefficients.

2.5. Fluorescence confocal microscopy

To complement back-extraction data, sodium fluorescein and Oregon Green 488 equilibrium partition coefficients were also obtained using two-photon fluorescence confocal microscopy following Kotsmar et al. [1]. A Carl Zeiss 510 LSM META NLO AxioImager confocal microscope (Jena, Germany) equipped with a Spectra-Physics MaiTai HP DeepSee Laser (Santa Clara, CA) was used for imaging at 780 nm. Fluorescence emission was detected through a Plan-Neofluar 10x/0.30 NA objective (Carl Zeiss GmbH) using a 500–550 nm emission filter.

Prior to the partition-coefficient measurement, swollen hydrogels were soaked in the pertinent aqueous solute-containing solution under magnetic stirring for at least 2 d at 400 rpm. Subsequently, a 1-mm thick layer of the aqueous solution in a small Petri dish was placed on the microscope platform and scanned in the vertical (z) direction at 5-μm intervals to a depth of at least 250 μm. Afterward, a solute-equilibrated 4 mm × 4 mm, 250-μm thick hydrogel was placed on a microscope slide (48300-047, VWR International, West Chester, PA, USA), covered (coverslip, 12-541-B, Fisher Scientific, Fair Lawn, New Jersey, USA), and placed on the microscope for scanning in the z-direction at the same laser power and detector setting as those during scanning of the bulk-aqueous solute solution. During each experiment, background fluorescence intensity was recorded and subtracted from solution and hydrogel signals. To test for reversibility, hydrogel samples were placed in solute-free solvent following equilibration. Loading concentration was varied over a factor of 10 with no change in the measured partition coefficient.

Fig. 1 displays typical fluorescence-confocal-microscopy images of sodium fluorescein in 0, 1, 10, 30, and 100 wt % MAA hydrogels at pH 7.4. The top half of each micrograph corresponds to the equilibrated aqueous solution, whereas the bottom half corresponds to the first 50 μm of the hydrogel, where measured fluorescence intensity is independent of sample depth (i.e., there is minimal signal attenuation over this depth [1,2]). In the concentration range studied, detected solute intensities inside the hydrogel and in the surrounding aqueous solution were proportional to dye concentration in all cases [1,2]. Thus, the partition coefficient is the ratio of solute intensity in the hydrogel to that in the aqueous-loading solution. Fig. 1 reveals that the partition coefficient of sodium fluorescein at pH 7.4 diminishes as the anionic MAA content of the copolymer hydrogel increases. At this pH, both sodium fluorescein and Oregon Green 488 completely desorb confirming reversible uptake. Accordingly, partition coefficients for sodium fluorescein and Oregon Green 488 from fluorescence confocal microscopy agree well with those obtained separately from back extraction at pH 7.4.

At pH 2, however, sodium fluorescein and Oregon Green 488 do not completely desorb even after 1 month of release. To quantify the amount of irreversibly adsorbed sodium fluorescein and Oregon Green 488 at pH 2, partition coefficients measured by fluorescence confocal microscopy in the loading direction were compared to those measured in release direction by back extraction. For 30 wt % MAA copolymer, where irreversible adsorption is most prevalent, k_i measured by back extraction was 35% lower, suggesting a maximum of 35% irreversible adsorption after 1 d of continued extraction. Partition coefficients reported here for sodium fluorescein and Oregon Green 488 are those obtained in the uptake direction.

2.6. Back extraction with UV/Vis-absorption spectrophotometry

Theophylline, caffeine, acetazolamide, and hydrocortisone equilibrium partition coefficients were obtained using back extraction or desorption [12,15,16,24,27] with UV/Vis-absorption spectrophotometry [18,22,24,25]. Solute-equilibrated hydrogels were removed from the loading solution, lightly blotted with Fisherbrand® weighing paper, and immediately placed into stirred aqueous solutions (400 rpm) of either PBS or HCl. Solute concentration was obtained as a function of time by periodically pipetting 1 mL of solvent into a 4-mm wide UV quartz cuvette (path length 10 mm), and measuring previously calibrated solution absorbance at 220–250 nm with an Ocean Optics spectrophotometer (Model ADC-1000, Dunedin, FL) and a deuterium UV/Vis DH-2000 light source. To maintain constant solution volume, the 1-mL samples were returned to the back-extraction solution following each concentration measurement.

The equilibrium partition coefficient, k_i, is calculated using the equilibrium back-extraction-solution concentration, C_i, [12]

$$k_i = \frac{C_i V}{C_{io} V^{gel}}, \quad (5)$$

where V is back-extraction-solution volume, V^{gel} is swollen-hydrogel volume, and C_{io} is equilibrium loading-solution concentration. Typical ratios of back-extraction-

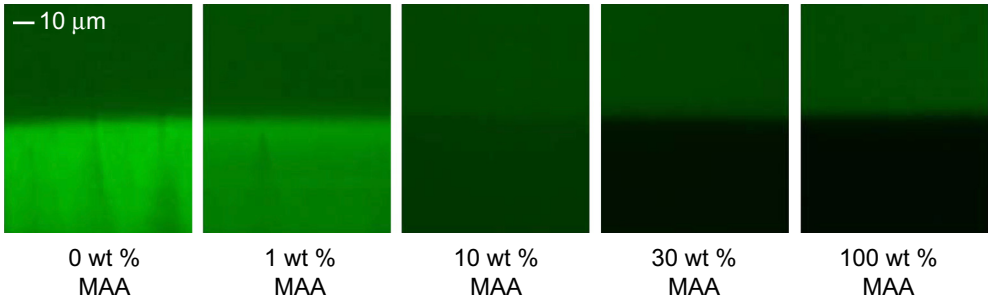

Fig. 1. Fluorescence-confocal-microscopy images of sodium fluorescein in 0, 1, 10, 30, and 100 wt % MAA hydrogels at pH 7.4. The top half of each micrograph corresponds to the equilibrated aqueous solution, whereas the bottom half corresponds to the first 50 μm of the hydrogel. The scale bar represents 10 μm in the vertical direction.

Table 2
Solute properties in aqueous PBS/HCl.[a]

Solute	Structure	pK_a	$D_o \times 10^6$ (cm^2/s)	a_{is} (nm)[b]	a_{is} (nm) lit.
Acetazolamide	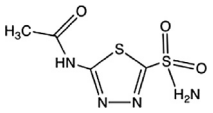	7.2, 8.8 [32]	6.1/4.8	0.41/0.50	0.40 [41,42]
Caffeine	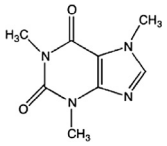	14.0 [38]	6.7/6.7	0.36/0.36	0.46 [42]
Hydrocortisone	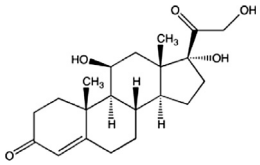	12.8 [39]	4.7/4.7	0.52/0.52	0.51 [42,43]
Oregon Green 488	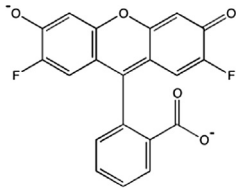	4.5, 4.8 [31]	4.0/3.9	0.62/0.54	0.60 [44]
Sodium fluorescein	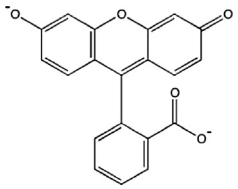	4.5, 6.5 [31]	4.0/3.9	0.62/0.56	0.58 [44]
Theophylline	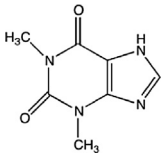	8.6 [40]	6.7/6.7	0.37/0.37	0.38 [24]

[a] Table entries separated by a diagonal correspond to measurement in aqueous PBS (pH 7.4) or in aqueous HCl (pH 2).
[b] Calculated from the Stokes–Einstein equation and measured aqueous diffusion coefficients.

to-hydrogel volume (V/V^{gel}) ranged from 20 to 2000, and were adjusted to provide precise calculation of k_i. Further increase of V/V^{gel} resulted in no significant change in k_i. To confirm constant dilute-solution partition coefficients, k_i, initial-solute-loading concentrations were increased and decreased by a factor of 4 resulting in less than a 10% difference.

To evaluate reversible adsorption for these four solutes, each hydrogel was loaded in aqueous HCl (pH 2) where solute adsorption is significant. The gels were then back extracted into aqueous PBS (pH 7.4) where solute adsorption is minimal. In all cases, k_i obtained by release into aqueous PBS agreed to within 5% of those obtained by back extraction into aqueous HCl (pH 2). It is thus reasonable to assert that theophylline, caffeine, acetazolamide, and hydrocortisone exhibit reversible uptake in all hydrogels and solution pH values studied here.

2.7. Solute size

To obtain the hydrodynamic radius of solute i, a_{is}, we first determined the corresponding dilute-aqueous bulk diffusion coefficient in a restricted diffusion cell [34] using UV/Vis absorption following Kotsmar et al. [1]. From the measured bulk diffusion coefficients, a_{is} was calculated from the Stokes–Einstein equation [1,2,34]. Solute concentrations were 4×10^{-4} M, in the range where light absorbance is linear with concentration. Bulk diffusion coefficients, D_o, were obtained from the constant slope of absorptivity versus time at later times [1,2,34]. Table 2 reports measured bulk aqueous diffusion coefficients and calculated Stokes–Einstein hydrodynamic radii, compared to available literature values. Agreement between literature and measurement is excellent.

3. Experimental results

Table 3 reports measured enhancement factors, $E_i \equiv k_i/\phi_1$, for acetazolamide, caffeine, hydrocortisone, Oregon Green 488, sodium fluorescein, and theophylline in HEMA/MAA hydrogels equilibrated in either PBS (pH 7.4) or HCl (pH 2) solutions. Hydrogel composition varies from 0 to 100 wt % MAA. At pH 7.4, all solutes exhibit $E_i > 1$ in 0 wt % MAA hydrogels (i.e., 100 wt % HEMA) owing to strong specific adsorption to the HEMA matrix, most significantly hydrocortisone. Conversely, for the nonionic solutes at pH 7.4 in 100 wt % polyelectrolyte MAA, near-unity enhancement factors suggest no specific adsorption to anionic MAA. As a result, E_i significantly decreases with addition of solute-non-interacting anionic MAA and with a corresponding decrease in the amount of specifically interacting HEMA copolymer.

Table 3 likewise reports solute enhancement factors in the HEMA/MAA hydrogels equilibrated in HCl (pH 2) solutions. All solutes and all hydrogels are neutral at pH 2; E_i is significantly greater than unity revealing strong specific adsorption to both HEMA and uncharged MAA polymers. The increase in E_i with addition of neutral MAA to the hydrogel (despite similar water

contents from 0 to 30 wt % MAA) indicates preferential adsorption on the uncharged MAA copolymer compared to that on the HEMA copolymer for all solutes. Accordingly, solute enhancement factors are greater in MAA-containing hydrogels equilibrated at pH 2 relative to those equilibrated at pH 7.4. At pH 2, all enhancement factors for 100 wt % MAA decline significantly compared to those for lower MAA-content hydrogels. This result discloses that the individual contributions to E_i are functions of water content. The large enhancement factors for neutral sodium fluorescein and Oregon Green 488 in Table 3 at pH 2 are commensurate with observed partial irreversibility.

Enhancement factors in Table 3 for dianionic sodium fluorescein ($pK_a \approx 4.5$, 6.5 [31]) and Oregon Green 488 ($pK_a \approx 4.5$, 4.8 [31]) in 100 wt % MAA ($pK_a \approx 5.2$ [30,35]) at pH 7.4 are a factor of six lower than those of the similar-sized neutral solutes. Thus, in addition to diminished specific solute interaction with the ionized MAA copolymer compared to neutral MAA groups, polymer-matrix charge density apparently plays a significant role in determining uptake of ionized solutes [35]. To investigate the possible effect of nonspecific electrostatic interaction on E_i, the ionic strength of the phosphate buffer solution (pH 7.4) was varied by adding NaCl to yield concentrations ranging from 0.02 to 1 M. Fig. 2 shows E_i versus ϕ_1 on a semi-logarithmic scale for sodium fluorescein in the HEMA/MAA hydrogels with 0.02 M (open triangles), 0.15 M (filled circles), and 1 M added aqueous NaCl (open squares). Lines in this figure correspond to theory described later. Despite a background-electrolyte Debye length of approximately 0.5 nm in PBS solution [1,2], we conclude that the significant rejection of dianionic sodium fluorescein reported in Table 3 for pH 7.4 results from electrostatic repulsion from anionic MAA groups. Added NaCl in Fig. 2 increases the enhancement factor of anionic sodium fluorescein because of increased screening of the negatively charged MAA copolymer.

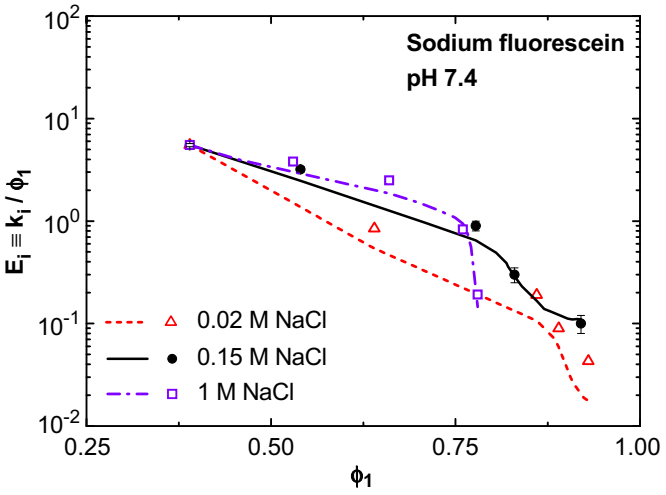

Fig. 2. Sodium-fluorescein enhancement factor, $E_i \equiv k_i/\phi_1$, as a function of water volume fraction, ϕ_1, in HEMA/MAA hydrogels equilibrated in phosphate buffer (pH 7.4) with 0.02 (open triangles), 0.15 (filled circles), and 1 M NaCl (open squares). Typical error bars are shown. Semi-logarithmic lines are drawn according to theory. Solid and dashed lines correspond to filled and open symbols, respectively.

4. Theory

Table 3 reports enhancement factors ranging from 0.1 to over 400 with substantial contributions from size exclusion, nonspecific electrostatic repulsion, and specific adsorption. At the dilute solute concentrations studied here, the adsorbing solutes follow Henry's law for uptake on the polymer chains [1]. Because solute concentrations are orders-of-magnitude smaller than that of the background electrolyte, there is no need to account for adsorption of the ionized-solute counterions.

Appendix A demonstrates that

$$E_i \equiv \frac{k_i}{\phi_1} = E_i^{ex} E_i^{el} \left(1 + \sum_j K_{ij} \phi_{2j} / \phi_1 \right) = E_i^{ex} E_i^{el} E_i^{ad}, \tag{6}$$

where ϕ_{2j} is the volume fraction of polymer component j, i.e., $\phi_2 \equiv 1 - \phi_1 = \sum \phi_{2j}$. The bracketed term in Eq. (6) represents the adsorption enhancement factor, $E_i^{ad} \equiv 1 + \sum K_{ij}\phi_{2j}/\phi_1$. Eq. (6) assumes that, at large dilution, each adsorbing solute does so independently on each copolymer of the hydrogel. With no specific adsorption ($K_{ij} = 0$), E_i reduces to that of size exclusion and electrostatic interaction. K_{ij} in Eq. (6) are unknown constants that are obtained here from independent experiment. Adsorption on the external surface of the hydrogel is not included because the area of external-surface polymer strands is miniscule compared to that of the internal chains.

The size-exclusion enhancement factor in Eq. (6), E_i^{ex}, follows from an extended Ogston mesh-size distribution [1,2,23,36]

$$E_i^{ex} = \exp\left\{ -4(1-\phi_1)\left[\left(a_{is}/a_f \right) \left(1 + a_{is}/a_f \right) \right] \right\}, \tag{7}$$

where a_{is} and a_f are solute and strand-fiber radii, respectively. Table 2 reports measured a_{is} for the six solutes studied. Following Kotsmar et al. [1], we take $a_f = 2$ nm, typical for HEMA/MAA hydrogels. For non-adsorbing, uncharged point solutes, Eqs. (6) and (7) correctly reduce to ideal partitioning (i.e., to $k_i = \phi_1$). As a_{is} increases, however, E_i^{ex} tends towards zero, because large solutes can access only a portion of the water-filled spaces in the hydrogel [1,2].

As outlined in Appendix A, the electrostatic enhancement factor for ionized solutes in Eq. (6), E_i^{el}, follows from equality of solute chemical potential in the hydrogel liquid-filled voids and that in the bulk aqueous solution including the electrostatic potentials of the two phases (i.e., Donnan theory [37])

$$E_i^{el} = \exp\left(-\frac{z_i F \psi}{RT} \right), \tag{8}$$

where z_i is the valence of solute i, F is Faraday's constant, and ψ is the Donnan electric potential difference between the hydrogel and

Table 3
Enhancement factors[a] with varying HEMA:MAA weight ratios in aqueous PBS/HCl.[b]

Hydrogel composition (HEMA:MAA)	Acetazolamide	Caffeine	Theophylline	Hydrocortisone	Oregon green 488 & sodium fluorescein
100:0	5.8/11.0	6.5/6.5	6.5/7.0	53.5/53.5	5.5/258.0
99:1	3.8/11.1	4.3/7.2	4.5/7.4	33.6/87.2	3.2/350.0
90:10	1.7/13.1	2.1/10.7	2.4/11.0	12.9/103.5	0.9/385.6
70:30	1.2/10.4	1.6/12.6	1.5/11.3	9.5/97.9	0.3/381.3
0:100	0.6/2.5	0.7/9.7	0.8/8.2	1.0/108.5	0.1/187.3

[a] Partition coefficients may be obtained by multiplying table entries by the corresponding water volume fractions listed in Table 1.
[b] Table entries separated by a diagonal correspond to solute enhancement factors measured in aqueous PBS (pH 7.4) or aqueous HCl (pH 2).

the bulk aqueous solution [37]. Eq. (8) predicts E_i^{el} once the unknown potential difference ψ is specified.

Because the concentration of solutes is dilute compared to that of the background electrolyte, ψ is set by the aqueous electrolyte ionic strength and pH, and the polyelectrolyte charge density. The indifferent electrolyte is assumed to be completely dissociated NaCl. As outlined in Appendix B, electroneutrality and phase equilibria for Na^+ and Cl^- ions provide an analytical expression for ψ

$$F\psi/RT = \ln\left[\sqrt{E^{ex}_{Na^+}/E^{ex}_{Cl^-} + \alpha^2} - \alpha\right], \quad (9)$$

where $\alpha \equiv C^{gel}_{MAA^-}/(2C^{bulk}_{NaCl}\,E^{ex}_{Cl^-}\,\phi_1)$, $C^{gel}_{MAA^-}$ is the molar concentration of charged MAA per total swollen hydrogel volume, F is Faraday's constant, R is the gas constant, and T is absolute temperature. In Eq. (9), C^{bulk}_{NaCl} is taken as the sum of the buffer (assumed a 1:1 electrolyte) and added NaCl concentrations in the bulk aqueous solution. $C^{gel}_{MAA^-}$ is related to the MAA copolymer weight fraction during synthesis, w_{MAA}, by $C^{gel}_{MAA^-} = w_{MAA} f_{[-]}(1-\phi_1)\,\rho_{dry}/M_{MAA}$, where M_{MAA} is MAA monomer molecular weight (86.1 g/mol [1]), ρ_{dry} is the mass density of dry polymer, and $f_{[-]}$ is the degree of ionization given by $f_{[-]} = 10^{-pK_a}/(10^{-pH} + 10^{-pK_a})$ [30]. The Donnan-based electrostatic enhancement factor does not account for specific ion binding of the solute (or background electrolyte) to the polymer strands.

Henry's adsorption constant for specifically adsorbed solute i on polymer component j, K_{ij}, includes all specific interactions with the polymer matrix. It is undetermined in Eqs. 6–9. Here subscript j denotes HEMA, anionic MAA (MAA- at pH 7.4), or nonionic MAA (MAA at pH 2). To obtain $K_{i\ HEMA}$, $K_{i\ MAA-}$, and $K_{i\ MAA}$, Eqs. 6–9 are fit to measured solute partition coefficients in 100 wt % HEMA, 100 wt % ionized MAA-, and 100 wt % unionized MAA hydrogels. Obtained values are listed in Table 4. As expected, none of the studied solutes adsorb onto the charged MAA polymer while adsorption on neutral MAA groups is larger than that on HEMA groups. Additionally, adsorption of the ionized forms of the solutes (pH 7.4) on HEMA is less than that of the corresponding neutral forms (pH 2).

5. Discussion

At pH 7.4, all solutes in Table 3 exhibit $E_i > 1$ for 0 wt % MAA hydrogels (i.e., 100 wt % HEMA) arising from strong specific adsorption to aqueous HEMA strands ($K_{i\ HEMA} > 0$ in Table 4). Except for hydrocortisone, Henry's adsorption constants for all solutes in Table 4 are similar in value (i.e., $6.5 < K_{i\ HEMA} < 9.2$) due to analogous hydrogen bonding between the solutes and the HEMA hydroxyl groups. For hydrocortisone, however, stronger adsorption to HEMA ($K_{i\ HEMA} = 83$) originates from a larger number of hydrogen-bond donors compared to the five other solutes. Conversely, at pH 7.4, the solutes display $E_i \sim 1$ in 100 wt % MAA^- resulting from lack of solute adsorption to anionic MAA moieties (i.e., $K_{i\ MAA-} = 0$).

At pH 2, however, all solutes exhibit $E_i > 1$ indicating strong specific adsorption to both HEMA and uncharged MAA copolymers ($K_{i\ HEMA} > 0$ and $K_{i\ MAA} > 0$ in Table 4). For nearly all solutes, $K_{i\ MAA} > K_{i\ HEMA}$ consistent with the lower pK_a of a carboxylic acid (MAA) compared to that of an alcohol (HEMA) [30]. For those solutes in Table 2 with $pK_a < 7.4$ (acetazolamide, sodium fluorescein, and Oregon Green 488), $K_{i\ HEMA}$ is larger when the solutes are neutral compared to their ionized states. $K_{i\ HEMA}$ and $K_{i\ MAA}$ for uncharged sodium fluorescein and Oregon Green 488 are an order of magnitude larger than those for the other solutes, commensurate with the observation of partial irreversibility [2].

With Henry's adsorption constants specified, Eqs. 6–9 predict E_i as a function of hydrogel composition, aqueous pH, and salinity.

Table 4
Henry's adsorption constant (dimensionless).

Solute	$K_{i\ HEMA}$[a]	$K_{i\ MAA-}$	$K_{i\ MAA}$[b]
Acetazolamide	6.5/13	0	5
Caffeine	9.2/9.2	0	30
Hydrocortisone	83/83	0	380
Oregon Green 488	8.6/~455	0	~730
Sodium fluorescein	8.5/~455	0	~730
Theophylline	7.5/7.5	0	21

[a] Table entries separated by a diagonal correspond to Henry's constant measured in aqueous PBS (pH 7.4) or in aqueous HCl (pH 2).
[b] In aqueous HCl (pH 2).

Solid and dashed lines in Fig. 3 compare predicted to measured (symbols) enhancement factors, E_i, as functions of water content, ϕ_1, for the six prototypical drugs in aqueous PBS buffer (pH 7.4). Lines are drawn using theory with no adjustable parameters. HEMA and charged MAA copolymer volume fractions follow from definition: $\phi_{2\ HEMA} = (1-w_{MAA})(1-\phi_1)$ and $\phi_{2\ MAA^-} = w_{MAA} f_{[-]}(1-\phi_1)$. In all cases, agreement between theory and experiment is excellent. For all solutes, E_i significantly decreases with incorporation of anionic MAA into the hydrogel, due to non-adsorption onto the charged MAA copolymer (i.e., $K_{i\ MAA-} = 0$). This lack of adsorption explains the general trend of decreasing E_i with increasing ϕ_1 seen in Fig. 3 and Table 3 for pH 7.4.

The magnitude of the enhancement factor is determined by the various contributions in Eq. (6). To illustrate, semi-logarithmic lines in Fig. 4 predict E_i^{ad} (dashed), E_i^{ex} (dotted), E_i^{el} (dash-dotted), and E_i (solid) for sodium fluorescein as a function of ϕ_1 in HEMA/MAA hydrogels equilibrated in aqueous PBS (pH 7.4). Filled circles denote measured enhancement factors. In 100 wt % HEMA (i.e., 0 wt % MAA) at pH 7.4, $E_i \sim 10$ arises from specific adsorption of 1:2 valence sodium fluorescein offsetting partial rejection due to size exclusion (i.e., $E_i^{ad} >> E_i^{ex}$ in Fig. 4). At pH 7.4, addition of anionic MAA copolymer increases ϕ_1 (see Table 1), gradually increasing E_i^{ex}, since sodium fluorescein accesses a larger fraction of the water-filled spaces [1]. Since E_i^{ad} decreases drastically compared to the slight increase in E_i^{ex} (typical for small solutes), E_i diminishes with addition of charged MAA. Sodium dianionic fluorescein (at pH 7.4) experiences additional rejection through Donnan electrostatic repulsion ($E_i^{el} < 1$) originating from the anionic MAA copolymer. Consequently, E_i decreases more dramatically with added MAA^- compared to E_i for similar-adsorbing nonionic solutes (e.g., theophylline in Table 3).

Fig. 2 also emphasizes the importance of E_i^{el} for determining enhancement factors of dilute, charged solutes. Lines in this figure correspond to Eqs. 6–9 for sodium fluorescein, as in Figs. 3 and 4. Increasing solution ionic strength increases the enhancement factor. The dependence of the enhancement factor on background ionic strength arises from the Donnan electrostatic potential, which is negative when the hydrogel is charged. Fig. 5 shows the calculated Donnan electric potential, expressed as $-F\psi/RT$, versus water content, ϕ_1, on a semi-logarithmic scale, corresponding to the enhancement factors predicted in Fig. 2. Lines are drawn using Eq. (9). As added NaCl concentration increases from 0.02 to 1 M, ψ decreases due to enhanced screening of the negative polyelectrolyte charge density by aqueous sodium chloride. As a result, E_i^{el} increases with addition of NaCl for a fixed polyelectrolyte charge density, giving rise to the increase in E_i seen in Fig. 2. Reduction in Donnan-potential confirms that ϕ_1 decreases with addition of NaCl for MAA-containing hydrogels at pH values above the pK_a [34].

Similar to Fig. 3, solid and dashed theory lines in Fig. 6 compare predicted to measured (symbols) enhancement factors, E_i, as a function of MAA copolymer content for the six prototypical drugs now in aqueous HCl (pH 2). Here, E_i is plotted against wt % MAA

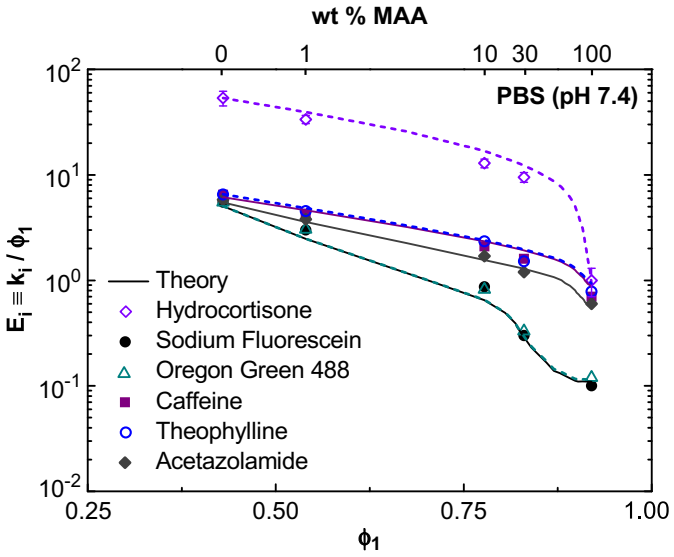

Fig. 3. Measured solute enhancement factors, $E_i \equiv k_i/\phi_1$, as functions of water volume fraction, ϕ_1, for hydrocortisone (open diamonds), sodium fluorescein (filled circles), Oregon Green 488 (open triangles), caffeine (filled squares), theophylline (open circles), and acetazolamide (filled diamonds) in HEMA/MAA hydrogels with varying wt % MAA in PBS (pH 7.4). Typical error bars are shown. Semi-logarithmic lines are drawn according to theory. Solid and dashed lines correspond to filled and open symbols, respectively. (For interpretation of the references to color in this figure legend, the reader is referred to the web version of this article.)

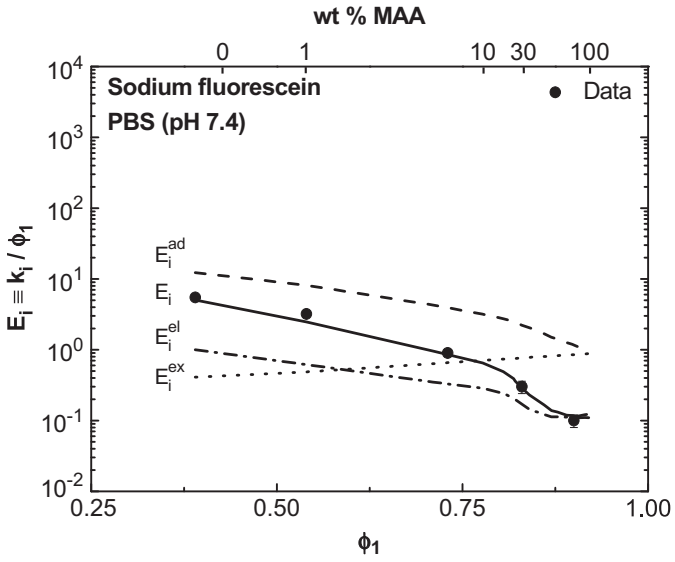

Fig. 4. Sodium-fluorescein enhancement factor versus water volume fraction, ϕ_1, in HEMA/MAA hydrogels equilibrated in PBS (pH 7.4). Semi-logarithmic lines are drawn according to theory. Solid, dashed, dotted, and dash-dotted lines correspond to E_i, E_i^{ad}, E_i^{ex}, and E_i^{el}. Symbols denote measured E_i in Table 3.

rather than ϕ_1, because addition of MAA at pH 2 yields a non-monotonic increase in ϕ_1 (see Table 1). Lines are drawn from Eqs. 6–9 with no adjustable parameters. The uncharged-MAA volume fraction is $\varphi_{2\,MAA} = w_{MAA}(1-\varphi_1)$. All solutes exhibit moderate Henry's adsorption constants in both 100 wt % HEMA and 100 wt % MAA at pH 2 (Table 4). Consequently, $E_i > 1$. Despite the very large loading partition coefficients of neutral sodium fluorescein and Oregon Green 488 and their partial irreversible adsorption, agreement between theory and experiment is excellent for all solutes.

The six studied solutes are neutral at pH 2; therefore, E_i is determined by a balance between size exclusion ($E_i^{ex} < 1$) and specific adsorption ($E_i^{ad} > 1$). Lines in Fig. 7 predict E_i^{ad} (dashed), E_i^{ex} (dotted), E_i^{el} (dash-dotted), and E_i (solid) for neutral sodium fluorescein as a function of MAA-copolymer content for HEMA/MAA hydrogels equilibrated in aqueous HCl (pH 2). In 100 wt % HEMA (i.e., 0 wt % MAA) at pH 2, $E_i > 1$ arises from significant specific adsorption offsetting rejection due to size exclusion (i.e., $E_i^{ad} >> E_i^{ex}$ in Fig. 7). Thus in Fig. 7 (and Fig. 6), E_i initially rises with incorporation of uncharged MAA into the hydrogel (corresponding to decreasing ϕ_1 in Table 1) due to an increase in E_i^{ad} that follows from an increase in the total polymer volume fraction ($1 - \phi_1$). E_i decreases with further addition of uncharged MAA (corresponding to increasing ϕ_1). The increased specific adsorption of solutes with increasing MAA content in Fig. 6 is offset by the overall increase in water content, similar to the decrease seen with MAA addition at pH 7.4. A slight maximum appears near 30 wt % MAA content.

The proposed model well predicts partitioning of drugs in copolymer hydrogels as a function of hydrogel composition, and aqueous pH and salinity. Theory assumes that in dilute solution the free energy of a dilute-solute-equilibrated hydrogel is additive in potential-of-mean-force molecular contributions or equivalently: $E_i \equiv E_i^{ex}\, E_i^{el}\, E_i^{ad}$. Several physical parameters are necessary to quantify the various individual enhancement factors. To establish E_i^{ex} in Eq. (7), required parameters are the hydrogel water content, ϕ_1, solute hydrodynamic radius, a_{is}, and fiber radius, a_f. As discussed elsewhere [1,2], ϕ_1, a_{is}, and a_f are conveniently obtained gravimetrically, from dilute bulk diffusion coefficients, and from oscillatory linear shear rheology, respectively. To obtain the Donnan electric potential needed in Eq. (9), and, therefore, E_i^{el} in Eq. (8), required hydrogel properties are the concentration of charged MAA carboxylate groups, $C^{gel}_{MAA^-}$, calculated from the MAA-copolymer weight fraction during synthesis and the degree of ionization, $f_{[-]}$. Finally, E_i^{ad} in Eq. (6) is established from ϕ_1, w_{MAA}, and the Henry's adsorption constants, $K_{ij} \cdot K_{ij}$ is obtained from fits of Eqs. 6–9 to measured solute partition coefficients in the corresponding homopolymer hydrogels. A more complete predictive theory demands *a priori* prediction of K_{ij} and ϕ_1.

6. Conclusions

We report measured and predicted equilibrium partition coefficients for six prototypical drugs in five soft-contact-lens-

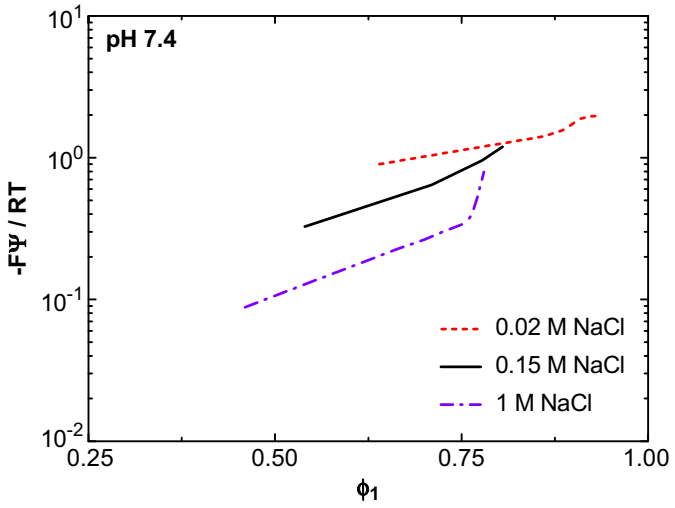

Fig. 5. Calculated dimensionless Donnan electric potential, $-F\psi/RT$, as a function of water volume fraction, ϕ_1, for MAA-containing HEMA/MAA hydrogels equilibrated in phosphate buffer (pH 7.4) with 0.02 (dashed line), 0.15 (solid line), and 1 M NaCl (dash-dotted line). Semi-logarithmic lines are drawn according to theory.

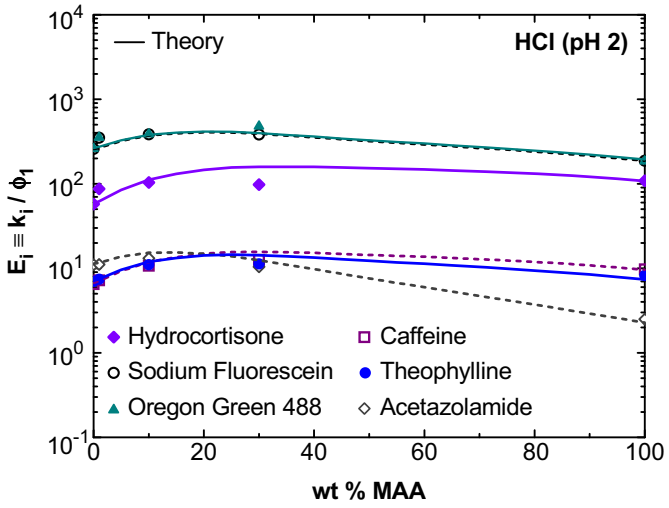

Fig. 6. Measured solute enhancement factors as functions of MAA copolymer content for hydrocortisone (filled diamonds), sodium fluorescein (open circles), Oregon Green 488 (filled triangles), caffeine (open squares), theophylline (filled circles), and acetazolamide (open diamonds) in HEMA/MAA hydrogels equilibrated in aqueous HCl (pH 2). Semi-logarithmic lines are drawn according to theory. Solid and dashed theory lines correspond to filled and open symbols, respectively. (For interpretation of the references to color in this figure legend, the reader is referred to the web version of this article.)

material hydrogels over a range of water contents. Partition coefficients were obtained using two-photon confocal microscopy and back extraction with UV/Vis-absorption spectrophotometry for acetazolamide, caffeine, hydrocortisone, Oregon Green 488, sodium fluorescein, and theophylline in 2-hydroxyethyl methacrylate/methacrylic acid (HEMA/MAA, $pK_a \approx 5.2$) copolymer hydrogels as functions of composition, aqueous pH (2 and 7.4), and salinity. Size exclusion, specific adsorption, and nonspecific electrostatic interaction control solute partitioning. To express deviation from ideal partitioning, we define an enhancement (or exclusion) factor, $E_i \equiv k_i/\phi_1$, where ϕ_1 is hydrogel water volume fraction [1]. At pH 7.4, all solutes exhibit $E_i > 1$ in 100 wt % HEMA hydrogels owing to strong specific adsorption to HEMA strands. As a result, E_i significantly decreases with addition of anionic MAA to the hydrogel due to non-interaction with the charged MAA. E_i for anionic sodium fluorescein, Oregon Green 488, and acetazolamide at pH 7.4, however, decreases more than those for similar-sized nonionic solutes. For divalent anionic sodium fluorescein, E_i increases significantly with rising NaCl concentration in phosphate buffer (from 0.15 to 1 M) due to screening of the dissociated carboxylate groups on the MAA copolymer. By assuming that the free energy of a solute-equilibrated hydrogel is additive in molecular contributions, we express the enhancement factor as a product of individual enhancement factors for size-exclusion (E_i^{ex}), nonspecific electrostatic interaction (E_i^{el}), and specific adsorption (E_i^{ad}) leading to $E_i \equiv E_i^{ex}\, E_i^{el}\, E_i^{ad}$. To obtain the individual enhancement factors, we employ an extended Ogston mesh-size distribution for E_i^{ex}, Donnan equilibrium for E_i^{el}, and Henry's law characterizing specific adsorption to the polymer chains for E_i^{ad}. In all cases, predicted enhancement factors demonstrate excellent agreement with experiment.

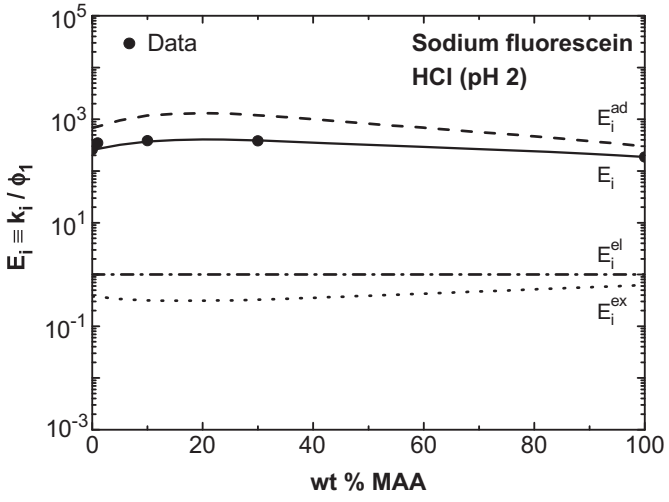

Fig. 7. Sodium-fluorescein enhancement factor as a function of MAA copolymer content in HEMA/MAA hydrogels equilibrated in aqueous HCl (pH 2). Semi-logarithmic lines are drawn according to theory. Solid, dashed, dotted, and dash-dotted lines correspond to E_i, E_i^{ad}, E_i^{ex}, and E_i^{el}. Symbols denote measured E_i in Table 3.

Nomenclature

a_{is}	hydrodynamic radius of solute i (nm)
a_f	strand-fiber radius (nm)
C_i	molar concentration of solute i (mol/L)
C_{io}	equilibrium loading-solution concentration (mol/L)
$C_{MAA^-}^{gel}$	concentration of charged MAA per total swollen hydrogel volume (mol/L)
C_{NaCl}^{bulk}	sum of the buffer and added NaCl concentrations in the bulk aqueous solution (mol/L)
D_o	bulk aqueous diffusion coefficient of solute (cm^2/s)
E_i	enhancement (or exclusion) factor
$f_{[-]}$	degree of ionization
F	Faraday's constant (C/mol)
k_i	equilibrium partition coefficient
K_a	acid dissociation constant
K_{ij}	Henry's constant for adsorption of solute i on copolymer strands j
m	mass (mg)
M_{MAA}	MAA monomer molecular weight (g/mol)
n_i	total solute adsorption density on the polymer matrix (moles of solute per volume of swollen polymer) (mol/L)
R	ideal gas constant (J/mol/K)
T	temperature (K)
V	back-extraction-solution volume (mL)
V^{gel}	swollen-hydrogel volume (mL)
w_{MAA}	MAA copolymer weight fraction in synthesis
z_i	valence of solute i

Greek letters

α	$C_{MAA^-}^{gel}/(2C_{NaCl}^{bulk}\, E_{Cl^-}^{ex}\, \phi_1)$ in Eq. (9)
ϕ	volume fraction (based on volume of swollen hydrogel)
μ_i	chemical potential of solute i (J/mol)
$\Delta\mu_i^{el}$	increment of ideal-dilute solute chemical potential in a polyelectrolyte hydrogel due to solute charge (J/mol)
$\Delta\mu_i^{ex}$	increment of ideal-dilute solute chemical potential in a hydrogel due to finite size (J/mol)
ρ_{dry}	mass density of dry polymer (g/cm^3)
ψ	Donnan electric potential (V)

Subscripts

1	water
2	polymer
i	solute
j	copolymer component

Superscripts

ad	adsorption
bulk	bulk aqueous solution
ex	size exclusion
el	electrostatic
gel	hydrogel
L	hydrogel liquid-filled spaces
o	ideal dilute-solution standard state for uncharged, point particles at unit concentration
oad	standard state for ideal adsorbed solute *i* at unit adsorption density on copolymer strands

Appendix A. Thermodynamics of partitioning

Consider a dilute aqueous weak-electrolyte solute of molar concentration, C_i^{bulk}, equilibrated with a copolymer hydrogel at solute concentration, C_i^{gel}, giving a partition coefficient $k_i \equiv C_i^{\text{gel}}/C_i^{\text{bulk}}$. Solute *i* resides in the liquid-filled spaces of the hydrogel and adsorbs onto the internal polymer strands so that [1,2]

$$C_i^{\text{gel}} \equiv \phi_1 C_i^L + \phi_2 n_i, \tag{A1}$$

where ϕ_1 and $\phi_2 \equiv 1 - \phi_1$ are the volume fractions of the liquid and polymer in the hydrogel, respectively, C_i^L is the liquid-space molar concentration (moles per liquid volume), and n_i is the total solute adsorption density on the polymer matrix (moles per polymer volume). Phase equilibrium demands that the solute chemical potential in the bulk aqueous phase equals that in the liquid interstices of the hydrogel which, in turn, equals that of the solute adsorbed on the polymer matrix

$$\mu_i^{\text{bulk}} = \mu_i^L = \mu_i^{ad} \tag{A2}$$

When a weak-electrolyte solute is ionized, chemical potentials in Eq. (A2) are replaced by electrochemical potentials [45].

The second expression in Eq. (A2) is evaluated by Henry's law for dilute-solute adsorption

$$\mu_i^o + RT \ln C_i^L = \mu_{ij}^{oad} + RT \ln n_{ij}, \tag{A3}$$

where n_{ij} is the adsorption density of solute *i* on copolymer *j* (i.e., moles of *i* per swollen volume of copolymer *j*), μ_i^o is the ideal dilute-solution standard-state chemical potential for uncharged, point particles *i* at unit concentration, and μ_{ij}^{oad} is the standard-state chemical potential for ideal adsorbed solute *i* at unit adsorption density on copolymer strands *j*. Henry's law for solute adsorption is rewritten from Eq. (A3) as

$$\phi_2 n_i \equiv \sum_j n_{ij}\phi_{2j} = C_i^L \sum_j K_{ij}\phi_{2\,j}, \tag{A4}$$

where ϕ_{2j} is the volume fraction of copolymer *j*. Individual copolymer Henry's adsorption constants for solute *i* are defined by $K_{ij} \equiv \exp[-(\mu_{ij}^{oad} - \mu_i^o)/RT]$.

The concentration of equilibrated solute in the liquid-filled spaces of the hydrogel, C_i^L, follows from the first equality of Eq. (A3)

$$\mu_i^o + RT \ln C_i^{\text{bulk}} = \mu_i^o + \Delta\mu_i^{ex} + \Delta\mu_i^{el} + RT \ln C_i^L, \tag{A5}$$

where $\Delta\mu_i^{ex}$ is the increment of ideal-dilute solute chemical potential in the hydrogel due to finite size, and $\Delta\mu_i^{el}$ is the increment of ideal-dilute solute chemical potential in a polyelectrolyte hydrogel due to solute charge. Similar to Eq. (A3), Eq. (A5) is rewritten as

$$C_i^L = E_i^{ex} E_i^{el} C_i^{\text{bulk}}, \tag{A6}$$

where $E_i^{ex} \equiv \exp(-\Delta\mu_i^{ex}/RT)$ is the finite-sized solute exclusion factor and $E_i^{el} \equiv \exp(-\Delta\mu_i^{el}/RT)$ is the finite-charge solute exclusion/enhancement factor. From Eq. (A5), the solute enhancement factors may be considered also as inverse activity coefficients in the gel.

Eqs. (1), (A1), (A4), and (A6) lead to Eq. (6) of the text. The size-exclusion enhancement factor E_i^{ex} is estimated from Eq. (7) while the electrical enhancement/exclusion factor E_i^{el} is obtained from Donnan exclusion in Eq. (8) [37]. Calculation of the Donnan potential is outlined in Appendix B.

Appendix B. Donnan potential

Since the aqueous solute concentration is much lower than that of the background electrolyte, the Donnan potential of the gel relative to the bulk solution, ψ, is set by the aqueous electrolyte ionic strength and pH, and the polyelectrolyte charge density. We approximate the buffer and acid electrolyte as completely dissociated, indifferent NaCl with bulk aqueous molar concentration $C_{\text{NaCl}}^{\text{bulk}}$.

Phase equilibrium demands that chloride (Cl^-) and sodium (Na^+) ion chemical potentials in the bulk aqueous phase equal those in the liquid-filled domains of the hydrogel. Because Donnan theory gives $\Delta\mu_i^{el} = z_i F\psi$ [37], Eqs. (A5) and (A6) for Cl^- reveal that

$$-\frac{F\psi}{RT} = \ln \frac{C_{\text{NaCl}}^{\text{bulk}} E_{Cl^-}^{ex}}{C_{Cl^-}^L}, \tag{B1}$$

where $C_{Cl^-}^L$ is the liquid-region chloride-ion molar concentration (moles of Cl^- per liquid volume) and ψ is the electric potential difference between the hydrogel and the bulk aqueous solution [37]. Eq. (B1) neglects specific adsorption of the background electrolyte to the polymer matrix. Consequently, addition of Eq. (A5) for Cl^- and Na^+ ions gives [37]

$$C_{Na^+}^L C_{Cl^-}^L = E_{Na^+}^{ex} E_{Cl^-}^{ex} \left(C_{\text{NaCl}}^{\text{bulk}}\right)^2, \tag{B2}$$

where $C_{\text{NaCl}}^{\text{bulk}} = C_{Cl^-}^{\text{bulk}} = C_{Na^+}^{\text{bulk}}$.

The hydrogel water phase contains mobile Na^+ and Cl^- ions and immobile charges MAA^- (dissociated MAA at pH 7.4). Electroneutrality requires that

$$C_{MAA^-}^{\text{gel}}/\phi_1 + C_{Cl^-}^L - C_{Na^+}^L = 0. \tag{B3}$$

Due to their very low concentrations compared to that of the background electrolyte, Eq. (B3) neglects the presence of H^+, OH^-, and dissociated solute *i*. Upon solving Eqs. (B2) and (B3) for $C_{Cl^-}^L$ and dividing by $C_{\text{NaCl}}^{\text{bulk}}$, we establish that

$$\frac{C_{Cl^-}^L}{C_{\text{NaCl}}^{\text{bulk}}} = \sqrt{\left(E_{Cl^-}^{ex} E_{Na^+}^{ex}\right)^2 + \left(\alpha\, E_{Cl^-}^{ex}\right)^2} - \alpha\, E_{Cl^-}^{ex}, \tag{B4}$$

where $\alpha \equiv C_{MAA^-}^{\text{gel}}/(2C_{\text{NaCl}}^{\text{bulk}}\, E_{Cl^-}^{ex}\, \phi_1)$. Finally, Eq. (9) of the text follows using Eq. (B1) to eliminate $C_{Cl^-}^L$ from Eq. (B4). Possible spatial non-uniformity of the electrostatic potential in the hydrogel is negligible at the background ionic strengths pertinent to this work [46].

References

[1] Kotsmar Cs, Sells T, Taylor N, Liu DE, Prausnitz JM, Radke CJ. Aqueous solute partitioning and mesh size in HEMA/MAA hydrogels. Macromolecules 2012;45(22):9177–87.

[2] Liu DE, Kotsmar Cs, Nguyen F, Sells T, Taylor N, Prausnitz JM, et al. Macromolecule sorption and diffusion in HEMA/MAA hydrogels. Ind Chem Eng Res 2013 [Accepted].
[3] Peppas NA, Bures P, Leobandung W, Ichikawa H. Hydrogels in pharmaceutical formulations. Eur J Pharm Biopharm 2000;50(1):27–46.
[4] D'Errico G, De Lellis N, Mangiapia G, Tedeschi A, Ortona O, Fusco S, et al. Structural and mechanical properties of UV-photo-cross-linked poly(*N*-vinyl-2-pyrrolidone) hydrogels. Biomacromolecules 2008;9(1):231–40.
[5] Lazzara MJ, Deen WM. Effects of concentration on the partitioning of macromolecule mixtures in agarose gels. J Colloid Interface Sci 2004;272(1):288–97.
[6] Mathur AM, Moorjani SK, Scranton AB. Method for synthesis of hydrogel networks: a review. J Macromol Sci C 1996;36(2):405–30.
[7] Kosto KB, Panuganti S, Deen WM. Equilibrium partitioning of Ficoll in composite hydrogels. J Colloid Interface Sci 2004;277(2):404–9.
[8] Peppas NA. Hydrogels and drug delivery. Biol Asp 1997;2(5):531–7.
[9] Gupta P, Vermani K, Garg S. Hydrogels: from controlled release to pH-responsive drug delivery. Drug Discov Today 2002;7(1):569–79.
[10] Güven O, Sen M, Karadag E, Saraydin D. A review on the radiation synthesis of copolymeric hydrogels for adsorption and separation processes. Radiat Phys Chem 1999;56(4):381–6.
[11] Kim JJ, Park K. Smart hydrogels for bioseparation. Bioseparation 1999;7(4–5):177–84.
[12] Guan L, Gonzalex-Himenez ME, Walowski C, Boushehri A, Prausnitz JM, Radke CJ. Permeability and partition coefficient of aqueous sodium chloride in soft contact lenses. J Appl Poly Sci 2011;122(3):1457–71.
[13] Luensmann D, Zhang F, Subbaraman L, Sheardown H, Jones L, Jones L. Localization of lysozyme sorption to conventional and silicone hydrogel contact lenses using confocal microscopy. Curr Eye Res 2009;34(8):683–97.
[14] Peng C-C, Burke MT, Chauhan A. Transport of topical anesthetics in vitamin E loaded silicone hydrogel contact lenses. Langmuir 2012;28(2):1478–87.
[15] Kim J, Chauhan A. Dexamethasone transport and ocular delivery from poly(hydroxyethyl methacrylate) gels. Int J Pharm 2008;353(1–2):205–22.
[16] Bangani LC, Leclerc J, Chauhan A. Lysozyme transport in p-HEMA hydrogel contact lenses. J Colloid Interface Sci 2012;386(1):441–50.
[17] Wu J, Sassi AP, Blanch HW, Prausnitz JM. Partitioning of proteins between an aqueous solution and a weakly-ionizable polyelectrolyte hydrogel. Polymer 1996;37(21):4803–80.
[18] Hirota N, Kumaki Y, Narita T, Gong JP, Osada Y. Effect of charge on protein diffusion in hydrogels. J Phys Chem B 2000;104(42):9898–903.
[19] Johnson EM, Berk DA, Jain RK, Deen WM. Diffusion and partitioning of proteins in charged agarose gels. Biophys J 2005;68(4):1561–8.
[20] Abbott NL, Blankschtein D, Hatton TA. Protein partitioning in two-phase aqueous polymer systems: 1. Novel physical pictures and a scaling-thermodynamic formulation. Macromolecules 1991;24(15):4334–48.
[21] Sassi AP, Blanch HW, Prausnitz JM. Characterization of size-exclusion effects in highly swollen hydrogels: correlation and prediction. J Appl Phys Sci 1998;59(8):1337–46.
[22] Stringer JL, Peppas NA. Diffusion of small molecular weight drugs in radiation-crosslinked poly(ethylene oxide) hydrogels. J Control Release 1996;42(2):195–202.
[23] Tong J, Anderson JL. Partitioning and diffusion of proteins and linear polymers in polyacrylamide gels. Biophys J 1996;70(3):1505–13.
[24] Bettini R, Colombo P, Peppas NA. Solubility effects on drug transport through pH-sensitive swelling-controlled release systems: transport of theophylline and metoclopramide monohydrochloride. J Control Release 1995;37(1–2):105–11.
[25] Merrill EW, Dennison KA, Sung C. Partitioning and diffusion of solutes in hydrogels of poly(ethylene oxide). Biomaterials 1993;14(15):1117–26.
[26] Ende MT, Peppas NA. Transport of ionizable drugs and proteins in cross-linked poly(acrylic acid) and poly(acrylic acid-co-2-hydroxethyl methacrylate) hydrogels: II. Diffusion and release studies. J Control Release 1997;48(1):47–56.
[27] Kapoor Y, Thomas JC, Tan G, John VT, Chauhan A. Surfactant-laden soft contact lenses for extended delivery of ophthalmic drugs. Biomaterials 2009;30(5):867–78.
[28] Ratner BD, Miller IF. Transport through crosslinked poly(2-hydroxyethyl methacrylate) hydrogel membranes. J Biomed Mater Res A 1973;7(4):353–67.
[29] Fatin-Rouge N, Milon A, Buffle J, Goulet RR, Tessier A. Diffusion and partitioning of solutes in agarose hydrogels: the relative influence of electrostatic and specific interactions. J Phys Chem B 2003;107(44):12126–37.
[30] Chan AW, Neufeld RJ. Modeling the controllable pH-responsive swelling and pore size of networked alginate based biomaterials. Biomaterials 2009;30(30):6119–29.
[31] Mottram LF, Boonyarattanakalin S, Kovel RE, Peterson BR. The Pennsylvania green fluorophore: a hybrid of Oregon green and Tokyo green for the construction of hydrophobic and pH-sensitive molecular probes. Org Lett 2006;8(4):581–4.
[32] Ribeiro A, Veiga F, Santos D, Torres-Labandeira JJ, Concheiro A, Alvarez-Lorenzo C. Bioinspired imprinted PHEMA-hydrogels for ocular delivery of carbonic anhydrase inhibitor drugs. Biomacromolecules 2011;12(3):701–9.
[33] Caykara T, Dogmus M, Kantoglu Ö. Network structure and swelling-shrinking behaviors of pH-sensitive poly(acrylamide-co-itaconic acid) hydrogels. J Polym Sci B Polym Phys 2004;42(13):2586–94.
[34] Newman J, Chapman TW. Restricted diffusion in binary solutions. AIChE J 1973;19(2):343–8.
[35] Khare AR, Peppas NA. Swelling/deswelling of anionic copolymer gels. Biomaterials 1995;16(7):559–67.
[36] Ogston AG. The spaces in a uniform suspension of fibres. Trans Faraday Soc 1958;54(0):1754–7.
[37] Overbeek JTh G. Colloid science I. New York: Elsevier Pub. Co; 1969. p. 189.
[38] Järvinen K, Akerman S, Svarfvar B, Tarvainen T, Viinikka P, Paronen P. Drug release from pH and ionic strength responsive poly(acrylic acid) grafted poly(vinylidenefluoride) membrane bags *in vitro*. Pharm Res 1998;15(5):802–5.
[39] Ghafourian T, Zandasrar P, Hamishekar H, Nokhodchi A. The effect of penetration enhancers on drug delivery through skin: a QSAR study. J Control Release 2004;99(1):113–25.
[40] Spataru N, Sarada BV, Tryk DA, Fujishima A. Anodic voltammetry of xanthine, theophylline, theobromine, and caffeine at conductive diamond electrodes and its analytical application. Electroanalysis 2002;14(11):721–8.
[41] Edwards A, Prausnitz MR. Fiber matrix model of sclera and corneal stroma for drug delivery to the eye. AIChE J 1998;44(1):214–25.
[42] Prausnitz MR, Noonan JS. Permeability of cornea, sclera, and conjunctiva: a literature analysis for drug delivery to the eye. J Pharm Sci 1998;87(12):1479–88.
[43] Johnson KA, Westermann-Clark GB, Shah DO. Diffusion of charged micelles through charged microporous membranes. Langmuir 1989;5(4):932–8.
[44] Müller CB, Loman A, Pacheco V, Koberling F, Willbold D, Richtering W, et al. Precise measurement of diffusion by multi-color dual-focus fluorescence correlation spectroscopy. EPL 2008;83(4). 46001-1-5.
[45] Newman J, Thomas-Alyea KE. Electrochemical systems. 3rd ed. New Jersey: John Wiley & Sons; 2004. p. 30–40.
[46] Victorov AI. Effect of morphology of a swollen ionomer gel on its salt uptake. Fluid Phase Equilib 2006;241(1–2):334–43.